ORGANOMETALLICS

Article

pubs.acs.org/Organometallics

Arene Ruthenium(II) Complexes as Low-Toxicity Inhibitor against the Proliferation, Migration, and Invasion of MDA-MB-231 Cells through Binding and Stabilizing *c-myc* G-Quadruplex DNA

Qiong Wu,[†] Kangdi Zheng,[‡] Siyan Liao,[§] Yang Ding,[‡] Yangqiu Li,*[,†] and Wenjie Mei*[,‡]

[†]Key Laboratory for Regenerative Medicine of Ministry of Education, Jinan University, Guangzhou, 510632, China

[‡]School of Pharmacy, Guangdong Pharmaceutical University, Guangzhou, 510006, China

[§]School of Pharmaceutical Sciences, Guangzhou Medical University, Guangzhou, 510180, China

Supporting Information

ABSTRACT: Arene Ru(II) complexes have long been extensively studied as potential inhibitors against the proliferation of tumor cells, but their behavior against the migration and invasion of tumor cells needs further research. In this work, a series of arene Ru(II) complexes, (η^6-C_6H_6)Ru(*p*-XPIP)Cl]Cl (X = H, **1**; F, **2**; Cl, **3**; Br, **4**; and I, **5**), have been synthesized, and their inhibitory activity against the migration and invasion of MDA-MB-231 breast cancer cells have been investigated. It is found that all of these complexes exhibit excellent inhibitory activity (IC_{50}) against the growth of MDA-MB-231 breast cancer cells, and the value of IC_{50} for **1**, **2**, **3**, **4**, and **5** is about >300, 52.6, 11.4, 45.5, and 59.1 μM, respectively. Further studies by wound-healing assay, FITC-geltain assay, and flow cytometry assay showed that **3** can apparently suppress the migration and invasion of MDA-MB-231 cells via the joint action of S-phase arrest and apoptosis. Moreover, the binding behavior of these arene Ru(II) complexes with *c-myc* G-quadruplex DNA has also been studied, and the results showed that these complexes can bind and stabilize *c-myc* G-quadruplex DNA in groove binding mode. Also, the low toxicity of **3** was confirmed by its low inhibitory activity against the growth of normal MCF-10A breast cells *in vitro* and the development of zebrafish embryos *in vivo*. In other words, these results indicated that synthetic arene Ru(II) complexes can be developed as low-toxicity agents against the proliferation, migration, and invasion of breast cancer cells.

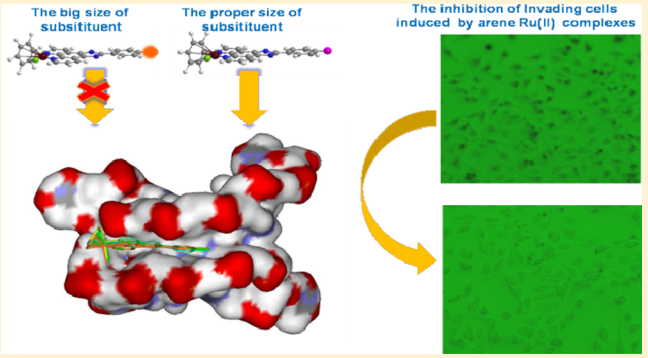

INTRODUCTION

Breast cancer has become an issue of growing concern in both research and clinical practice, as it is prevalent among younger women. Despite the advances that have taken place in the past decade, including the development of novel molecular targeted agents, cytotoxic chemotherapy remains the mainstay of breast cancer treatment.[1] It is so difficult to treat breast cancer owing to the heterogeneity of the disease, especially for triple-negative patients.[2] Consequently, the search for effective drugs to inhibit the proliferation and invasion of breast cancer has become a challenge. In recent years, arene Ru(II) complexes have attracted more attention in chemotherapy because of their low toxicity and excellent inhibitory activity against tumor cell migration and invasion. Numerous arene Ru complexes have already been designed. The *in vitro* and *in vivo* inhibitory activities of these complexes, as well as their underlying mechanisms and binding behavior to DNA molecules, have been extensively investigated. RAPTA-B ([Ru(η^6-C_6H_6)(pta)-Cl_2]) and RAPTA-C ([Ru(η^6-*p*-$C_6H_4Me^iPr$)(pta)Cl_2]) blocked tumor metastasis of a CBA mouse model for human breast cancer by preventing angiogenesis.[3] In addition, the arene Ru(II) complex RM175 ([(η^6-biphenyl)Ru(ethylenediamine)-Cl]$^+$) inhibited tumor metastasis *in vivo* and blocked migration and invasion through enhancing cell−cell readhesion and down-regulated the matrix metalloproteinases (MMPs).[4]

On the other hand, the *c-myc* oncogene is related to the proliferation, cell cycle arrest, metastasis, and invasion of tumor cells; this gene is located near a promoter region and is overexpressed in tumor cells, but has low expression in normal cells.[5] Recent studies showed that the G-rich promoter of the *c-myc* oncogene can form a G-quadruplex structure via a Hoogesten hydrogen bond in the presence of K^+ and Na^+ ions.[6]

Complexes that can bind and stabilize G-quadruplex DNA usually exhibit excellent inhibitory activity against the growth of tumor cells. For example, porphyrin and quindoline inhibit various tumor cells by stabilizing the *c-myc* G-quadruplex DNA.[7] Therrien reported that arene Ru(II) complexes with porphyrin can strongly bind to tetrastranded DNA structures to inhibit the telomerase enzyme.[8] Barone found that Schiff-base

Received: October 1, 2015

DOI: 10.1021/acs.organomet.5b00820
Organometallics XXXX, XXX, XXX−XXX

metal (Ni, Cu, and Zn) complexes can selectively bind to G4 DNA and stabilize G4 structures.[9] The latest studies by our team also found that arene Ru(II) complexes greatly inhibit the migration and invasion of breast cancer cells by blocking the formation of invadopodia, but these complexes have low toxicity to normal cells.[10] Moreover, these complexes can bind and stabilize the G-quadruplex structure of *c-myc*, thereby causing the down-regulation of *c-myc* and the induction of S-phase arrest in tumor cells.[11]

In the current study, a class of arene Ru(II) complexes of $(\eta^6$-$C_6H_6)$Ru(*p*-XPIP)Cl]Cl with X = **1** (H), **2** (F), **3** (Cl), **4** (Br), and **5** (I) were synthesized via microwave irradiation under controlled temperatures (Figure 1). Single-crystal X-ray

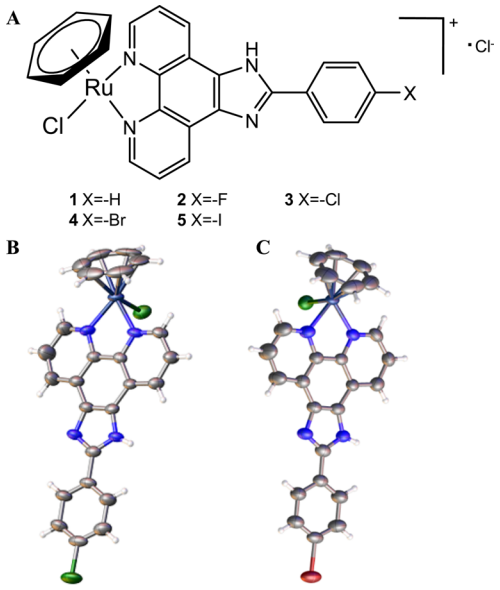

Figure 1. (A) Synthetic arene Ru(II) complexes coordinated by phenanthrolineimidazole ligands. The ball-and-stick diagrams of the arene Ru **3** (B) and **4** (C). For clarity, the solvent molecules and the counteranions are omitted. CCDC nos.: 1030971 (**3**); 1030972 (**4**).

diffraction analysis was conducted to confirm that these complexes have a typical "piano stool" structure. These complexes can bind to the *c-myc* G-quadruplex DNA in the groove-binding mode, with the following levels of binding affinity: **1** < **2** < **3** > **4** > **5**. Further study showed that these complexes, especially **3**, can inhibit the growth, migration, and invasion of MDA-MB-231 cells through the joint action of S-phase arrest and apoptosis. The low toxicity on developing zebrafish embryos was also investigated *in vivo*. Therefore, these arene Ru(II) complexes can be developed into potential low-toxicity agents against the metastasis of breast cancer for chemotherapy.

MATERIALS AND METHODS

Chemicals. Ruthenium(III) chloride hydrate was obtained from Mitsuwa Chemicals. 1,10-Phenanthroline monohydrate, 1,3-cyclohexadiene, benzaldehyde, 4-fluorobenzaldehyde, 4-chlorobenzaldehyde, 4-bromobenzaldehyde, and 4-iodobenzaldehyde were purchased from Aldrich. All chemicals, including the solvents, were obtained from commercial vendors and used as received. 1,10-Phenanthroline-5,6-diode was prepared by a similar method reported in literature. The binuclear arene Ru(II) complex $[(\eta^6$-$C_6H_6)RuCl_2]_2$ was prepared according to the literature. The *c-myc* G-quadruplex DNA (5′-TGGGGAGGGTGGGGAGGGTGGGGAAGG-3′) was purchased from Sangon Biotech (Shanghai) Co., Ltd. The G-quadruplex conformation was formed by denaturation at 90 °C for 5 min followed by renaturation at 4 °C for 24 h, as stipulated by methods in other studies. All aqueous solutions were prepared with double-distilled water.

Instruments. The arene Ru(II) complexes were synthesized using an Anton Paar GmbH monowave 300 microwave reactor. The elemental analyses for C, H, and N were performed with a Carlo-Erba CHNO-S microanalyzer. The IR spectra (KBr disk, 400−4000 cm^{-1}) were obtained with a PerkinElmer 1320 spectrometer. The ^1H NMR and ^{13}C NMR spectra were recorded in DMSO-d_6 with a Bruker DRX2500 spectrometer operating at room temperature. The electronic absorption spectra were recorded with a Shimadzu UV-2550 spectrophotometer. The steady-state emission spectra were recorded with an RF-5301 fluorescence spectrophotometer. The circular dichroism (CD) spectra were recorded with a Jasco J810 CD spectrophotometer.

Synthesis of 2-Phenylimidazole[4,5*f*][1,10]phenanthroline (PIP). PIP was prepared by a method similar to that described in the literature with some modifications.[12] Phenanthroline-5,6-dione (347 mg, 1.6 mmol), benzaldehyde (169.6 mg, 1.6 mmol), and ammonium acetate (2.53 g) were dissolved in 20 mL of acetic acid. The mixture was irradiated under microwave at 110 °C for 30 min. Subsequently, 20 mL of water was added, and the pH value was adjusted to 7.0 by adding ammonia at room temperature. A large amount of yellow precipitate was obtained after filtration, and this precipitate was dried under vacuum. The products were purified by silica gel chromatography with ethanol as the eluent to obtain the desired compound with a yield of 93.2%.

Synthesis of 2-(4-Fluorophenyl)imidazole[4,5*f*][1,10]-phenanthroline (*p*-FPIP). *p*-FPIP was prepared from 1,10-phenanthroline-5,6-dione (347 mg, 1.6 mmol) and 4-fluorobenzaldehyde (198 mg, 1.6 mmol) using a method similar to that described in the literature. The yield was 95.6%.

Synthesis of 2-(4-Chlorophenyl)imidazole[4,5*f*][1,10]-phenanthroline (*p*-ClPIP). *p*-ClPIP was prepared from 1,10-phenanthroline-5,6-dione (347 mg, 1.6 mmol) and 4-chlorobenzaldehyde (224 mg, 1.6 mmol) using a method similar to that described in the literature. The yield was 91.7%.

Synthesis of 2-(4-Bromophenyl)imidazole[4,5*f*][1,10]-phenanthroline (*p*-BrPIP). *p*-BrPIP was prepared from 1,10-phenanthroline-5,6-dione (347 mg, 1.6 mmol) and 4-bromobenzaldehyde (294 mg, 1.6 mmol) using a method similar to that described in the literature. The yield was 92.1%.

Synthesis of 2-(4-Iodophenyl)imidazole[4,5*f*][1,10]-phenanthroline (*p*-IPIP). *p*-IPIP was prepared from 1,10-phenanthroline-5,6-dione (347 mg, 1.6 mmol) and 4-iodobenzaldehyde (371.1 mg, 1.6 mmol) using a method similar to that described in the literature. The yield was 93.2%.

Synthesis of the Arene Ru Complex $[(\eta^6$-$C_6H_6)$Ru(PIP)Cl]Cl (1). **1** was prepared according to the literature, but with some modifications.[13] A mixture of $[(C_6H_6)RuCl_2]Cl_2$ (75 mg, 0.15 mmol) and phenanthroline derivatives (88.8 mg, 0.3 mmol) in dichloromethane (20 mL) was heated at 60 °C for 30 min under microwave irradiation. A yellow precipitate was obtained after rotary evaporation, and this precipitate was purified by recrystallization from distilled water. The yield was 138.4 mg (90.3%). ESI-MS (in MeOH, *m*/*z*): 525.4 ($[M - Cl]^+$). Anal. Calcd for $C_{25}H_{18}C_{l2}N_4Ru{\cdot}4H_2O{\cdot}CH_3OH$: 48.00 C, 4.65 H, 8.61 N. Found: 47.59 C, 3.93 H, 8.66 N. UV−vis in MeOH [λ_{max}, nm (ε, × 10^4 M^{-1} cm^{-1})]: 253 (4.34), 293 (2.69). IR (in KBr; ν_{max}, cm^{-1}): 3419.89, 3059.49, 2911.03, 1622.31, 1549.82, 1459.29, 1435.44, 1407.28, 1365.08, 1104.63, 810.28, 772.63, 704.29, 627.82. ^1H NMR (500 MHz, DMSO): δ 9.95 (d, J = 5.2 Hz, 2H), 9.39 (s, 2H), 8.44 (J = 7.5 Hz, 2H), 8.17 (dd, 2H), 7.61 (t, J = 7.4 Hz, 2H), 7.55 (t, J = 7.2 Hz, 1H), 6.34 (s, 6H). ^{13}C NMR (126 MHz, DMSO): δ 154.35 (s), 53.52 (s), 143.70 (s), 133.13 (s), 130.67 (s), 130.03 (s), 129.53 (s), 129.10 (s), 128.54 (s), 127.18 (s), 126.43 (s).

Synthesis of the Arene Ru Complex $[(\eta^6$-$C_6H_6)$Ru(*p*-FPIP)Cl]Cl (2). **2** was prepared using the method described above, but with *p*-FPIP (94.2 mg, 0.3 mmol) instead of PIP. The yield was 144.1 mg

DOI: 10.1021/acs.organomet.5b00820
Organometallics XXXX, XXX, XXX−XXX

(90.8%). ESI-MS (in MeOH, m/z): 529.01 ([M − Cl]$^+$). Anal. Calcd for $C_{25}H_{17}FCl_2N_4Ru{\cdot}3H_2O{\cdot}CH_3OH$: 47.51 C, 4.58 H, 8.21 N. Found: 47.21 C, 3.42 H, 8.23 N. UV−vis in MeOH [λ_{max}, nm (ε, × 10^4 M^{-1} cm^{-1})]: 279 (4.17). IR (in KBr; ν_{max}, cm^{-1}): 3367.25, 3040.54, 2929.72, 2894.18, 2854.55, 2814.15, 2768.62, 2692.98, 1623.98, 1601.05, 1508.91, 1473.49, 1363.55, 1322.12, 1276.81, 1200.16, 1145.57, 1105.58, 1082.08, 813.12, 722.28, 627.48, 549.5. ^{1}H NMR (500 MHz, DMSO-d_6, δ/ppm): 9.93 (dd, J = 5.3, 1.1 Hz, 2H), 9.32 (s, 2H), 8.46 (dd, J = 8.9, 5.4 Hz, 2H), 8.16 (dd, J = 8.3, 5.3 Hz, 2H), 7.46 (t, J = 8.9 Hz, 2H), 6.31 (s, 6H). ^{13}C NMR (126 MHz, DMSO): δ 155.94 (s), 153.97 (s), 145.24 (s), 134.66 (s), 131.11 (s), 131.07 (s), 128.03 (s), 127.96 (s), 118.14 (s), 117.98 (s), 88.79 (s).

Synthesis of the Arene Ru Complex [(η^6-C_6H_6)Ru(p-ClPIP)Cl]Cl (3). **3** was prepared in a similar method to that described above, but with p-ClPIP (99.3 mg, 0.3 mmol) in the place of PIP. The yield was 147.8 mg (90.4%). ESI-MS (in MeOH, m/z): 546.1 ([M − Cl]$^+$). Anal. Calcd for $C_{25}H_{17}C_{l3}N_4Ru{\cdot}5H_2O$: 44.75 C, 4.06 H, 8.35 N. Found: 44.88 C, 3.73 H, 8.62 N. UV−visible in MeOH [λ_{max}, nm (ε, × 10^4 M^{-1} cm^{-1})]: 283 (3.37). IR (in KBr; ν_{max}, cm^{-1}): 3419.05, 3054.23, 1623.57, 1607.86, 1508.19, 1475.49, 1463.02, 1453.52, 1421.22, 1405.86, 1364.57, 1319.22, 1101.76, 950.89, 836.23, 809.5, 723.76. ^{1}H NMR (500 MHz, DMSO-d_6, δ/ppm): 14.73 (s, 1H), 9.96 (dd, J = 8.5, 1.5 Hz 2H), 9.36 (s, 2H), 9.21 (s, 2H), 8.39 (d, J = 8.6 Hz, 2H), 8.22 (s, 2H), 7.74 (d, J = 8.6 Hz, 2H), 6.33 (s, 6H). ^{13}C NMR (126 MHz, DMSO): δ 148.76 (s), 144.25 (s), 143.51 (s), 132.51 (s), 129.82 (s), 129.61 (s), 129.26 (s), 128.49 (s), 125.85 (s), 115.69 (s), 87.13 (s).

Synthesis of the Arene Ru Complex [(η^6-C_6H_6)Ru(p-BrPIP)Cl]Cl (4). **4** was prepared in a similar method to that described above, but with p-BrPIP (112.2 mg, 0.3 mmol) in the place of PIP. The yield was 100.8 mg (89.8%). ESI-MS (in MeOH, m/z): 590.9 ([M − Cl]$^+$). Anal. Calcd for $C_{25}H_{17}Cl_2BrN_4Ru{\cdot}2H_2O{\cdot}CH_3OH$: 45.04 C, 3.63 H, 8.08 N. Found: 45.24 C, 3.27 H, 8.01 N. UV−vis in MeOH [λ_{max}, nm (ε, × 10^4 M^{-1} cm^{-1})]: 281 (3.03). IR (in KBr; ν_{max}, cm^{-1}): 3368.04, 3036.31, 2928.99, 2853.53, 2768.92, 2691.32, 1626.69, 1603.49, 1460.40, 1405.55, 1364.18, 1303.2, 1069.4, 1009.05, 832.2, 812.32, 727.28, 627.11. ^{1}H NMR (500 MHz, DMSO-d_6, δ, ppm): 9.93 (dd, J = 5.3, 1.1 Hz, 2H), 8.31 (d, J = 8.6 Hz, 2H), 8.18 (dd, J = 8.1, 5.5 Hz, 2H), 7.84 (d, J = 8.6 Hz, 2H), 7.34 (s, 2H), 6.30 (s, 6H). ^{13}C NMR (126 MHz, DMSO): δ 150.45 (s), 133.93 (s), 131.31 (s), 130.17 (s), 127.35 (s), 124.51 (s), 88.59 (s).

Synthesis of Arene Ru Complexes [(η^6-C_6H_6)Ru(p-IPIP)Cl]Cl (5). **5** was prepared as described above, but with p-IPIP (126.2 mg, 0.3 mmol) in the place of PIP. The yield was 168.7 mg (88.3%). ESI-MS (in MeOH), m/z): 636.9 ([M − Cl]$^+$). Anal. Calcd for $C_{25}H_{17}C_{l2}IN_4Ru{\cdot}10H_2O{\cdot}17CH_3OH$: 36.10 C, 7.57 H, 4.01 N. Found: 36.42 C, 3.56 H, 4.02 N. UV−vis in MeOH [λ_{max}, nm (ε, × 10^4 M^{-1} cm^{-1})]: 284 (3.16). IR (in KBr; ν_{max}, cm^{-1}): 3423.78, 2922.01, 1627.28, 1431.97, 1384.49, 1261.01, 1026.95, 803.2, 721.25, 535.09. ^{1}H NMR (500 MHz, DMSO-d_6, δ, ppm): δ 9.94 (d, J = 4.4 Hz, 2H), 9.33 (s, 2H), 8.19 (dd, 4H), 8.01 (t, J = 22.4 Hz, 2H), 6.34 (s, 6H). ^{13}C NMR (101 MHz, DMSO): δ 193.25 (s), 153.20 (s), 143.30 (s), 138.64 (s), 137.81 (s), 136.59 (s), 132.77 (s), 131.40 (s), 128.89 (s), 125.62 (s), 88.13 (s).

X-ray Crystallography. The single crystals of **3** and **4** were obtained by dissolving the powders in mixed solutions of distilled water and dimethylformamide. X-ray diffraction measurements were performed on a Rigaku R-AXIS SPIDER image plate diffractometer with graphite-monochromated Mo Kα radiation (λ = 0.710 73 Å). Absorption correction was applied with the SADABS program.[14] The structured solution and the full-matrix least-squares refinement based on F^2 for **3** and **4** were obtained with the SHELXS 97 and SHELXL 97 program packages, respectively. Anisotropic thermal parameters were applied to all non-hydrogen atoms. All hydrogen atoms were included in the calculated positions and refined with isotropic thermal parameters based on those of the parent atoms.

Cell Lines and Culture. Human cancer cell lines, including human breast cancer MDA-MB-231, human breast adenocarcinoma MCF-7, human hepatocarcinoma HepG2, human esophageal carcinoma EC-1, and human breast epithelial MCF-10A were purchased from American Type Culture Collection (ATCC, Manassas, VA, USA). The cell lines of MDA-MB-231, MCF-7, HepG2, and EC-1 were maintained in DMEM with fetal bovine serum (10%), penicillin (100 units/mL), and streptomycin (50 units/mL) at 37 °C in a CO_2 incubator (95% relative humidity, 5% CO_2). MCF-10A cells were maintained in DMEM with horse serum (10%), penicillin (100 units/mL), streptomycin (50 units/mL), EGF (20 ng/mL), hydrocortisone (0.5ug/mL), cholera toxin (100 ng/mL), and insulin (10ug/mL) at 37 °C in a CO_2 incubator (95% relative humidity, 5% CO_2).

MTT Assay. Cell viability was determined by measuring the ability of cells to transform MTT to a purple formazan dye. Cells were seeded in 96-well tissue culture plates for 24 h. The cells were then incubated with the test compounds at different concentrations for 72 h. After incubation, 20 μL of the MTT solution (5 mg mL^{-1}) in phosphate-buffered saline was added to each well, followed by incubation for an additional 5 h.[15] The medium was aspirated and replaced with 150 μL of DMSO per well to dissolve the formed formazan salt. The color intensity of the formazan solution, which reflects the cell growth conditions, was measured at 570 nm using a microplate spectrophotometer (SpectroAmax 250).

Wound-Healing Assay. Cells were seeded in six-well tissue culture plates, which were respectively marked on the back (1 × 10^5 cells per well) until the monolayer cells covered more than 80% of the bottom of the culture plate. A line was then scratched on the culture using a tip (200 μL pipet) orthogonal to the mark on the plate. Subsequently, these cells were incubated with the test compounds at different concentrations (0 and 10 μM) for 48 h. Migrating cells were observed in the same visual field every 12 h for 2 d.[16] Using Slidebook and Excel software, the average migration rate and the end-to-end distance of cell trajectory were calculated based on 10 fields of view for each cell type.

Fluorescein Isothiocyanate (FITC)-Conjugated Gelatin Invasion Assay. The FITC-gelatin invasion assay was performed according to the manufacturer's instructions (Invitrogen). Briefly, coverslips (18 mm in diameter) were coated with 50 μg mL^{-1} poly-L-lysine for 20 min at room temperature, washed with phosphate-buffered saline (PBS), fixed with 0.5% glutaraldehyde for 15 min, and rewashed with PBS three times. After washing, the coverslips were inverted on a drop of 0.2% FITC-conjugated gelatin in PBS containing 2.0% sucrose, incubated for 10 min at room temperature, washed with PBS thrice, quenched with sodium borohydride (5 mg mL^{-1}) for 3 min, and finally incubated in 2 mL of complete medium for 2 h.[17] Cells (2 × 10^5 per well) with different concentrations of **3** (0, 1, 2, and 5 μM) were plated onto the FITC-gelatin-coated coverslips and incubated at 37 °C for 12 h. The FITC-gelatin degradation status was evaluated and photographed with a laser confocal microscope.

Flow Cytometry Analysis. Cells were seeded in six-well tissue culture plates (1 × 10^5 cells per well), and the apoptosis rate and the cell cycle arrest were analyzed by flow cytometry as previously described.[16] After incubating with different concentration of **3** (0, 10, 20, and 40 μM) for 24 h, cells were trypsinized, washed with PBS, and fixed with 70% ethanol overnight at 4 °C. The fixed cells were washed with PBS and stained with propidium iodide (PI) for 15 min in the dark, and the cell cycle arrest was analyzed with an Epics XL-MCL flow cytometer (Beckman Coulter, Miami, FL, USA). Treated or untreated cells were trypsinized, washed with PBS, and costained with annexin-V and PI for 10 min, respectively. The apoptosis of cells was analyzed with an Epics XL-MCL flow cytometer (Beckman Coulter).

Molecular Docking. The theoretical calculation of the binding mode and binding site of arene Ru(II) complexes in *c-myc* G-quadruplex DNA was carried out by using the Lamarckian genetic algorithm local search method with Auto-Dock 4.2.A as previously described. Only chain A was maintained after the removal of other subunits form the crystallographic structure of the *c-myc* G-quadruplex DNA downloaded from the Protein Data Bank (PDBID: 2L7 V), and the Gasteiger charge and other parameters were assigned by using AutoDock tools. The size of the grid box was set to 126 × 126 × 126 points and centered with (x, y, z) = (2.579, −0.627, and −4.749) on *c-myc* G-quadruplex DNA. A total of 50 separate dockings were performed with maximum energy evaluations up to 2.5 × 10^7. The

DOI: 10.1021/acs.organomet.5b00820
Organometallics XXXX, XXX, XXX−XXX

Table 1. Cytotoxic Effects of Arene Ru(II) Complexes on Human Cancer and Normal Cell Lines and the Corresponding Lipophilicity

	$IC_{50}/\mu M$					
compd	MDA-MB-231	MCF-7	EC-1	HepG2	MCF-10A	log *P*
1	>300	>300		289.3 ± 13.4		−1.26
2	52.6 ± 1.3	297.9 ± 7.1	>300	92.8 ± 5.3		−1.16
3	11.4 ± 2.8	88.7 ± 3.1	105.7 ± 4.7	137.4 ± 2.6	209.3 ± 10.7	−0.14
4	45.5 ± 3.4	194.5 ± 4.8	36.4 ± 8.3	68.2 ± 3.5		0.02
5	59.1 ± 1.4	>300		179.3 ± 3.2		−0.474
cisplatin	36.1 ± 4.7	3.0 ± 4.4	174.1 ± 8.2	13.6 ± 1.4		−0.412

most probable binding conformation was selected according to the most cluster members and the lowest binding free energy.[18]

UV−Vis Spectra. The absorption titration of the Ru(II) complex in Tris-HCl buffer was performed with a fixed complex concentration to which increments of the DNA stock solution were added.[19] In general, the absorption spectra of arene Ru(II) complexes **1**, **2**, **3**, **4**, and **5** were recorded with increasing amounts of *c-myc* G-quadruplex DNA until the absorbance intensity of the arene Ru(II) complexes became constant. The concentration of the complex solution was 20 μM, and the *c-myc* G-quadruplex DNA was added in increments. The complex−DNA solutions were incubated for 3 min before the absorption spectra were recorded. The intrinsic binding constant K_b of the arene Ru(II) complex to DNA was calculated from the following equation:

$$(\varepsilon_a - \varepsilon_f)/(\varepsilon_b - \varepsilon_f) = [b - (b^2 - 2K^2C_t[\mathrm{DNA}/S)]^{1/2}/2KC_t \quad (1)$$

$$b = 1 + KC_t + K/2S \quad (2)$$

EB-Quenching Experiments. Fluorescence quenching of the ethidium bromide (EB) + *c-myc* G-quadruplex system can be used for a compound with an affinity to DNA regardless of its binding mode. This method measures only the ability of a compound to affect the EB fluorescence intensity in the EB + *c-myc* G-quadruplex system. Two mechanisms have been proposed to account for the quenching, as follows: the replacement of EB fluorophores and/or electron transfer. The EB-DNA complex excited at 530 nm showed strong fluorescence at 600 nm.[15] According to the quenching curve, we can draw the preliminary conclusion that the complex can competitively bind to DNA with EB.

CD Spectra. To obtain further information, we recorded the CD spectra of DNA modified by complex **3**. The respective CD spectral characteristics were compared for CT-DNA in the absence and presence of complex **3**. Complex **3** has no intrinsic CD signals because it is achiral; thus, any CD signal at higher than 300 nm can be attributed to the interaction of this complex with DNA.[13] This increasing reduction was similar to that observed when DNA was under identical conditions modified by cisplatin or its ineffective isomer, transplatin.

CD Melting Point. Typical CD melting curves were obtained by following the change in their ellipticity as a function of temperature at 262 or 292 nm. The solutions were heated at a rate of 0.1 °C min^{-1} using free strained quartz cuvettes with a path length of 0.1 or 1.0 cm, thereby resulting in the collection of two data points at C. The analysis of the CD melting curves was performed with standard procedures.[10]

ESI-MS Analysis. Several noncovalent interactions between nucleic acids and small ligands are biologically important processes. ESI-MS is recognized as a useful tool in the characterization of such binding. The stoichiometry and selectivity of the binding of small molecules to oligonucleotides can usually be obtained with minimal sample consumption. For G-quadruplex DNA, the mass spectra are usually obtained with an LCQ ion trap mass spectrometer equipped with a heated capillary electrospray source or a Q-TOF mass spectrometer equipped with a Z-spray source. Both instruments can be operated in the negative ion mode.[20]

Ecotoxicology Test of Zebrafish Embryos. Zebrafish embryos were provided by the Southern Medical University. Zebrafish embryos were incubated in 24-well plates with 1 mL solutions containing different concentrations (0, 2, 4, 8, 16, and 32 μM) of complex **3** in water. The hatching and growth of the zebrafish embryos without and with complex **3** were observed every 24 h with an inverted microscopy.[21] The relevant ethical protocols used for the *in vivo* study for zebrafish embryos were followed by the relevant laws.

RESULTS AND DISCUSSION

Synthesis and Characterization. Arene Ru(II) complexes **1** to **5** were prepared from $[(C_6H_6)RuCl_2]_2$ and the respective ligands (PIP, *p*-FPIP, *p*-ClPIP, *p*-BrPIP, and *p*-IPIP) at 60 °C under microwave irradiation for 30 min in a Pyrex vessel with a high yield range of 88−91%, which was markedly higher than that in conventional synthesis methods.[22] The crystallite is prepared through dissolvent crystallization. The molecular structure of the complexes was established by single-crystal X-ray structural analysis of the chloride salts (Figure 1). The selected bond distances and bond angles are listed in Tables S1 and S2 of the Supporting Information. The arene Ru(II) complexes adopt a classic "piano stool" structure, as evidenced by the ∼90° bond angles for N(1)−Ru(1)−Cl(1) (85.54(13)°) and N(2)−Ru(1)−Cl(1) (85.14(11)°) of **2** and N(3)−Ru(1)−Cl(1) (85.39(14)°) and N(4)−Ru(1)−Cl(1) (84.32(12)°) of **3**. The Ru(II) atom was bound to the benzene ring, with an average Ru−C distance of 2.183(7) and 2.181(7) Å, whereas the average distance of Ru(II) to the two chelating nitrogen atoms was 2.089(5) and 2.082(5) Å, respectively. The clear characterization of the structure of the complexes supported the elucidation of its possible anticancer mechanisms.[23]

Inhibitory Activities of Arene Ru Complexes *in Vitro*. The antiproliferative activities of the synthetic Ru(II) complexes against various human cancer cell lines and normal MCF-10A human cells were evaluated by using the MTT assay. The inhibitory activities (IC_{50}) of these synthetic Ru(II) complexes after 72 h of treatment are summarized in Table 1.

As shown in Table 1, the antiproliferative effects of these complexes are cell-line specific. The most active complex (**3**) displayed the highest inhibitory activity against MDA-MB-231 human breast cancer cells with an IC_{50} value of 11.4 μM. This value is approximately 3 times lower than that of cisplatin.[24] **3** showed low toxicity to normal MCF-10A human cells with an IC_{50} value of approximately 209.3 μM.

Lipophilicity often plays a major role in biology. Thus, we determined the lipophilicity partition coefficient. The lipophilicity partition coefficients for **1**, **2**, **3**, **4**, and **5** were approximately −1.26, −1.16, −0.14, 0.02, and −0.474, respectively. This result is reasonable given that molecular polarity changes with the size of the atom. Therefore, we concluded that atomic size plays a key role in DNA-binding

DOI: 10.1021/acs.organomet.5b00820
Organometallics XXXX, XXX, XXX−XXX

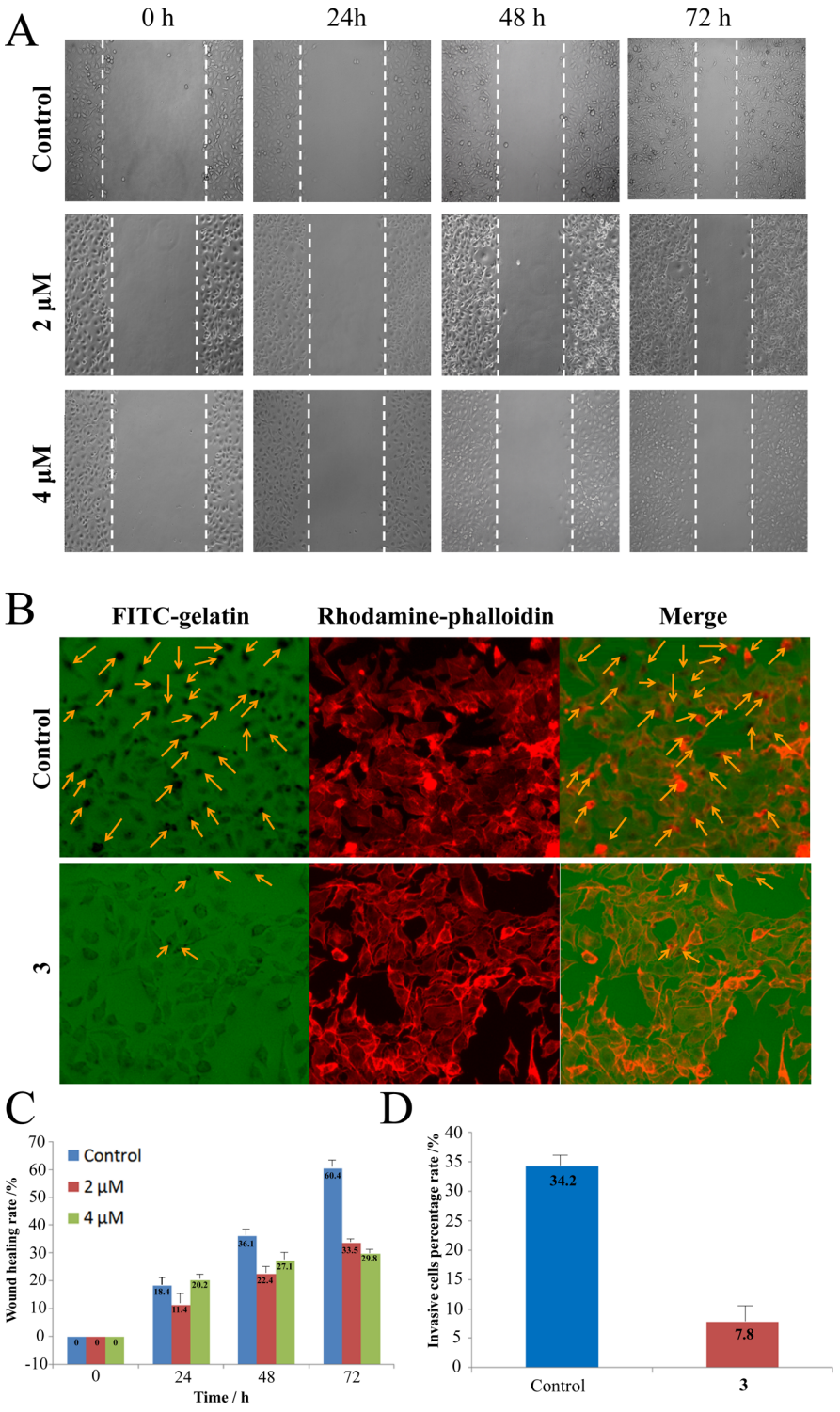

Figure 2. Inhibition of migration and invasion of MDA-MB-231 cells by **3** *in vitro*. (A) The wound-healing assay was used to evaluate the migration of MDA-MB-231 cells after treatment with **3** (0, 2, and 4 μM) and DMEM without FBS. Cells were wounded and monitored with a microscope every 12 h. The migration was determined by the rate of cells filling the scratched area. (B) The invasion of MDA-MB-231 cells was blocked by **3** (2 μM). The whole view of many MDA-MB-231 cells, the number of black holes observed without **3**, and those treated with **3**. Cell cytoskeletons were dyed by rhodamine-conjugated phalloidin. The dark area in the FITC-gelatin was identified as the position degraded by MDA-MB-231 cells. (C) Wound-healing rate of MDA-MB-231 cells induced by **3**. (D) Number of invasive cells reduced by **3**.

behavior and in the anticancer activity of these arene Ru(II) complexes.

Migration and Invasion of MDA-MB-231 Cells Is Inhibited by the Joint Action of S-Phase Arrest and Apoptosis. The inhibitory activity of **3** against the migration and invasion of MDA-MB-231 cells was further evaluated by wound-healing and FITC-gelatin assays (Figure 2).

As shown in Figure 2A, MDA-MB-231 cells treated without drugs showed an obvious decrease in the distance of wound closure at 72 h, but with the addition of **3**, a notable inhibition

DOI: 10.1021/acs.organomet.5b00820
Organometallics XXXX, XXX, XXX−XXX

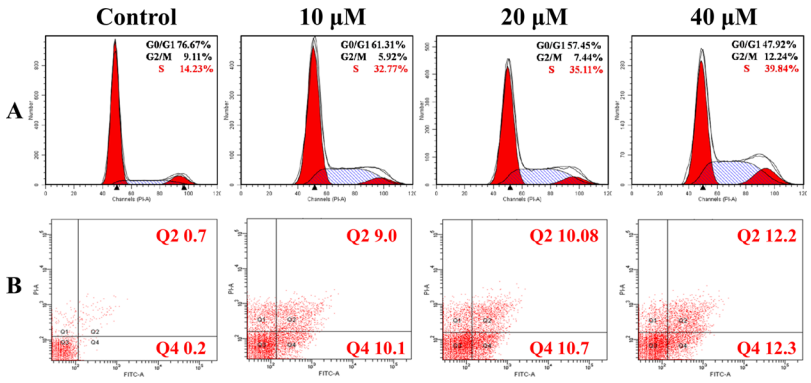

Figure 3. (A) S-phase arrest of MDA-MB-231 cells induced by **3**. (B) Apoptosis of MDA-MB-231 cells induced by **3**.

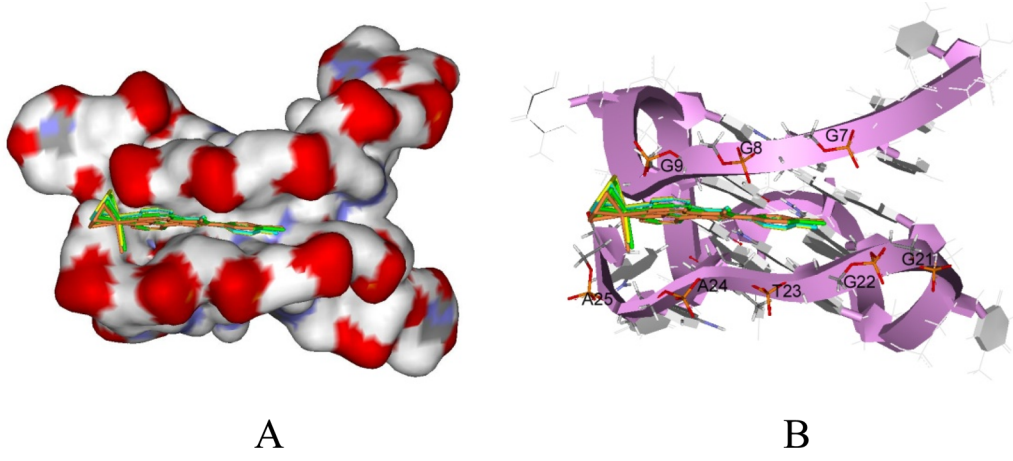

Figure 4. Binding mode (A) and binding site (B) of **1** (yellow), **2** (cyan), **3** (orange), and **4** (green) with *c-myc* G4 DNA calculated by molecular docking.

of wound closure was observed; the treatment had a dosage-dependent effect compared with the control cells, which spontaneously migrated as the distance obviously decreased. Less than confluent cultures showed the decreasing wound-healing rate of MDA-MB-231 cells with increasing concentration of **3**, thereby indicating that **3** effectively inhibited the migration of MDA-MB-231 cells even at low concentrations (Figure 2C).[25] The FITC-gelatin invasion assay is usually applied to observe the number of invasive tumor cells. In general, cells with high invasion rates can form invadopodia to release MMPs, which degrade the FITC-gelatin. Consequently, dark holes (nonfluorescent areas) can be observed in the FITC-gelatin. The higher number of dark holes implied greater invasiveness of the tumor cells. As shown in Figure 2B, numerous black holes could be counted in the FITC-gelatin for cells that were not treated with **3**. After exposure to **3**, the number of black holes obviously decreased, thereby indicating that the invasive effect of MDA-MB-231 cells was markedly inhibited.[26] These results proved that arene Ru complexes can effectively inhibit the invasion of MDA-MB-231 cells.[27]

Subsequently, flow cytometry was performed to examine the inhibitory activity of **3** against the growth of MDA-MB-231 cells. Specifically, this activity resulted from apoptosis, cell cycle arrest, or the joint action of both modes (Figure 3).

As shown in Figure 6, the exposure of MDA-MB-231 cells to 10, 20, and 40 μM **3** for 24 h triggered a significant increase in the number of cells under S-phase arrest and in the induction of cell apoptosis.[28] These results revealed that the growth inhibition induced by **3** was caused by the joint action of the S-phase arrest and apoptosis of breast cancer cells (Figure 3A and B).

Binding Studies with *c-myc* G-Quadruplex DNA. Moreover, the promoter of the *c-myc* oncogene plays a key role in regulating the proliferation, apoptosis, cell cycle arrest, invasion, and metastasis of tumor cells, which is G-riched DNA sequences and can form the G-quadruplex structure.[29] Molecular calculation was first performed to clarify the binding of the Ru(II) complexes with *c-myc* G-quadruplex DNA because the *c-myc* G-quadruplex has been extensively investigated as a potential target of antitumor agents. The results are presented in Figure 4.

According to the results of the docking calculations, all the as-prepared complexes, except **5**, were able to bind to the groove constructed by base pairs A6-G9 and G21-A25 in *c-myc* G-quadruplex DNA.[30] In addition, the G8 guanine in the *c-myc* G-quadruplex DNA forms a hydrogen bond with the N−H atom of the imidazole ring to provide additional stability. The binding energy of these complexes was calculated.

The binding of these complexes was further confirmed by electronic titration. The results are illustrated in Figure 5. As shown in Figure 5, obvious hypochromic events occurred at the characterized metal-to-ligand charge transition and the interligand charge (IL) transition of these complexes upon the addition of *c-myc* G-quadruplex DNA. The intrinsic binding constant (K_b) was calculated according to the decay IL absorption. The values of K_b for **1**, **2**, **3**, **4**, and **5** were

DOI: 10.1021/acs.organomet.5b00820
Organometallics XXXX, XXX, XXX−XXX

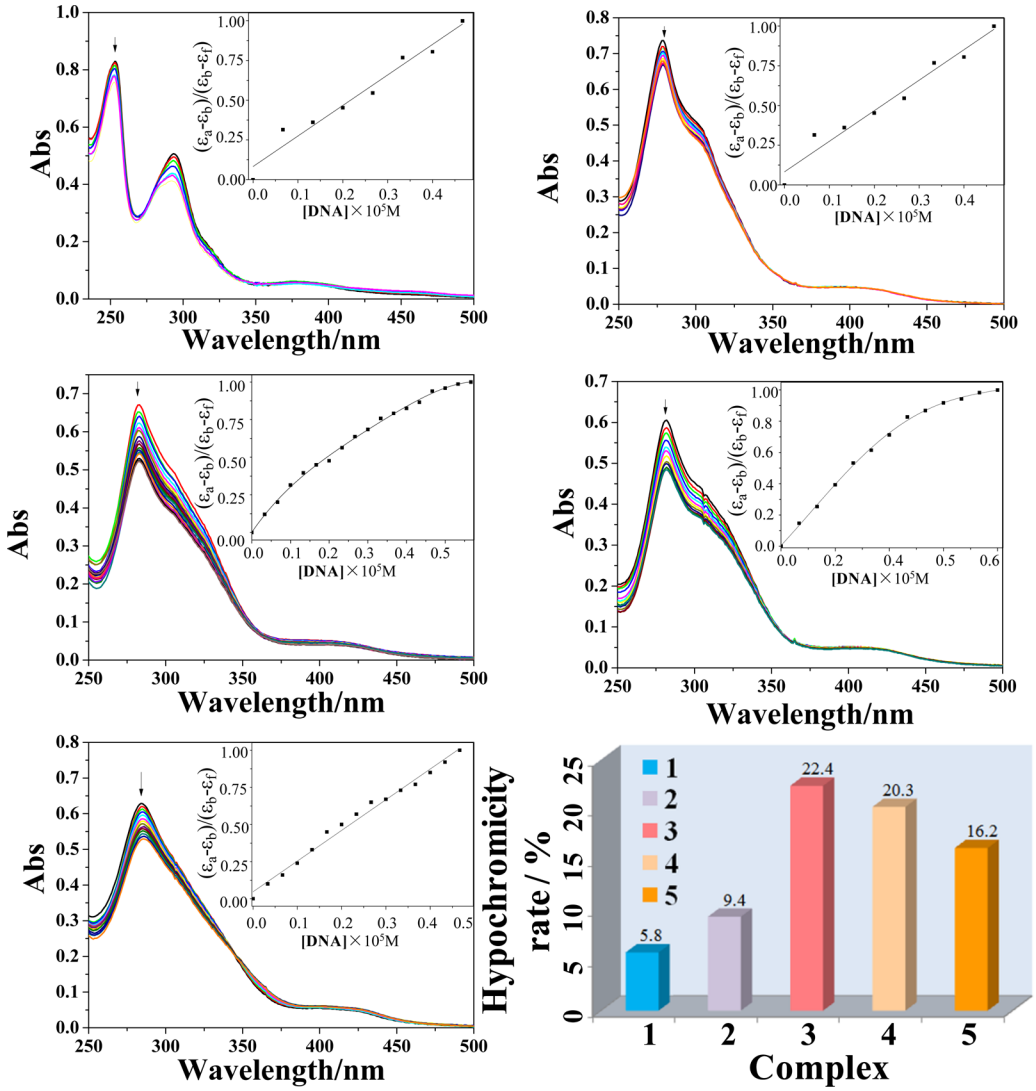

Figure 5. Electronic absorption spectra of **1** (A), **2** (B), **3** (C), **4** (D), and **5** (E) in the absence and presence of *c-myc* G-quadruplex DNA, [Ru] = 20 μ M. (F) Hypochromicity rate of **1**, **2**, **3**, **4**, and **5** of *c-myc* G-quadruplex DNA.

approximately 0.43, 0.77, 53.0, 51.0, and 4.5 × 10^5 M^{-1}, respectively. These results are consistent with the molecular docking calculations, thereby indicating that the change of the atomic radii in the substituent groups of main ligands determined the binding affinity of the complexes with G-quadruplex DNA.[31]

Furthermore, the ESI-MS, emission, and CD spectra were used to demonstrate the binding behavior of **3** with *c-myc* G-quadruplex DNA, as shown in Figure 6.

Initially, ESI-MS analysis was utilized to clarify the interaction of **3** with *c-myc* G-quadruplex DNA. The molecular weight of *c-myc* G-quadruplex DNA is M = 6970. The different anion peaks (m/e) attributed to $[M + 6Cl^-]^{6-}$, $[M + 6Cl^- - H^+]^{7-}$, $[M + 4Cl^- - 4H^+]^{8-}$, $[M + 5Cl^- - 4H^+]^{9-}$, $[M + 4Cl^- - 6H^+]^{10-}$, and $[M + 4Cl^- - 7H^+]^{11-}$ were observed at m/z 1197.3, 1026.4, 889.0, 792.1, 712.0, and 646.6, respectively (Figure 6A). When complex **3** was added to the solution, new anion peaks for $[M + 3^+ + 6Cl^- - 2H^+]^{7-}$, $[M + 3^+ + 5Cl^- - 4H^+]^{8-}$, and $[M + 3^+ + 3Cl -- 7H^+]^{9-}$ appeared at m/z 1101.4, 960.8, and 847.6, respectively (Figure 6B). These results indicated that complex **3** can bind with *c-myc* G-quadruplex DNA with high affinity.[32]

Moreover, the fluorescence quenching experiment of the EB-*c-myc* system was also conducted. The EB-DNA system displayed strong fluorescence at 600 nm when it was excited at 350 nm. Upon the addition of **3**, the fluorescence intensity of the EB-*c-myc* solution obviously decreased (Figure 5C and D). At [**3**] = 6 μM, the relative fluorescence strength (I/I_0) of the EB-*c-myc* solution in the presence of **3** was 0.37, thereby implying that **3** can competitively interact with the *c-myc* G-quadruplex DNA by replacing EB.[33]

The CD spectra also confirmed that **3** can strongly bind to the *c-myc* G-quadruplex DNA. A strong positive signal of *c-myc* G-quadruplex DNA was observed in the range 250−300 nm with the maximum signal at 263 nm, whereas a negative signal in the range 200−250 nm was noted with the maximum signal at 245 nm. As shown in Figure 6E, the CD signal of the *c-myc* G-quadruplex DNA markedly decreased with increasing concentration of **3**. Then, the strength of the positive signal decreased by 35.1%, and that of the negative signal decreased by 27.6%. The interaction of the complex with *c-myc* G-quadruplex DNA was accompanied by a conformational change, which contributed to the change or the induction of

DOI: 10.1021/acs.organomet.5b00820
Organometallics XXXX, XXX, XXX−XXX

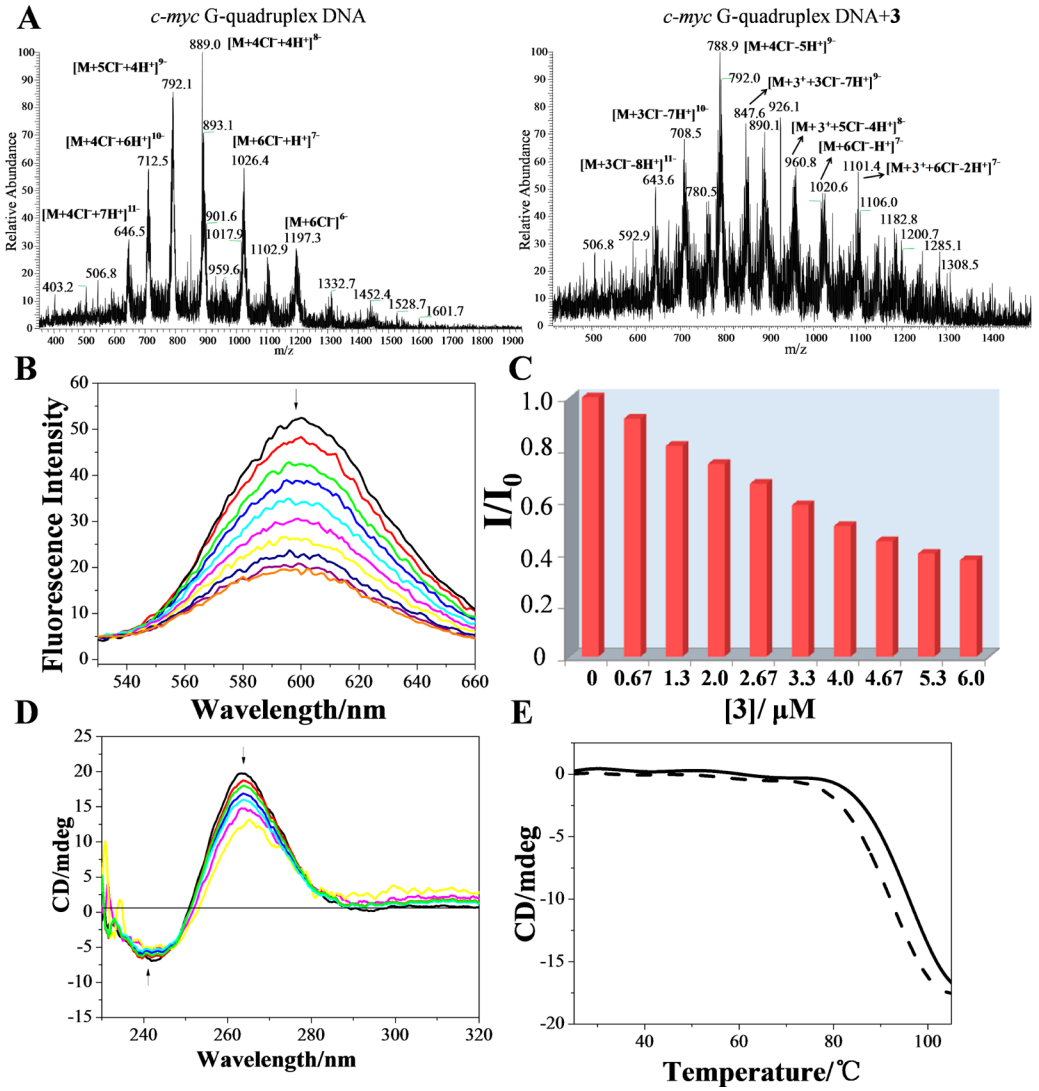

Figure 6. (A) ESI-MS analysis of *c-myc* G-quadruplex DNA without **3** (left) and with **3** (right) in NH_4Ac/MeOH (12:5) buffer, [*c-myc*] = 300 μM, [**3**] = 300 μM. (B) Emission spectra of EB (16 μM) and *c-myc* (2 μM) in 10 mM Tris-HCl and 100 mM KCl buffer (pH 7.4) in the addition **3**. (C) Trend change of emission spectra with increasing **3**. (D) CD titration spectra of *c-myc* (2 μM) at increasing **3** in 10 mM Tris-HCl and 100 mM KCl buffer (pH 7.4). (E) Typical CD melting curves of *c-myc* (2 μM) and *c-myc* (2 μM) + [Ru] (10 μM) in 10 mM Tris-HCl and 100 mM KCl buffer (pH 7.4), conducted at 263 nm.

the CD signal.[34] These results further confirmed that arene Ru(II) complexes can bind to *c-myc* G-quadruplex DNA.

To further evaluate the stability of *c-myc* G-quadruplex DNA with Ru(II) complexes, a CD melting assay was conducted to investigate the melting changes of complex **3** on the *c-myc* G-quadruplex DNA. As shown in Figure 6F, the T_M of *c-myc* was approximately 90.2 °C, whereas the T_M of the *c-myc* G-quadruplex DNA with complex **3** was approximately 94.5 °C (ΔT_M = 4.3 °C), thereby indicating that complex **3** can interact and stabilize the conformation of the *c-myc* G-quadruplex DNA by binding to the groove of *c-myc* G-quadruplex via $\pi-\pi$ stacking.[13,35]

Toxicity Assessments of Developing Zebrafish Embryos *in Vivo*. The *in vivo* toxicity assessments of **3** were conducted on developing zebrafish embryos. The zebrafish model is one of the most promising models for evaluating the toxicity of drugs. This effectiveness can be attributed to their high homology with human DNA, high reproductive rate, short growth period, and high fertility. The results are shown in Figure 7.

As shown in Figure 7B, without treatment with **3**, all the zebrafish embryos developed into juvenile zebrafish. After exposure to **3** at low concentrations, most of the zebrafish embryos developed into juvenile zebrafish, and the cumulative hatching rate was more than 80% after 96 h (Figure 7B). The lethality rate of **3** to zebrafish embryos was lower than 50% after 96 h (Figure 7C). When treated with high Ru(II) complex concentration ([Ru] of 16 and 32 μM) for 24 h, an incomplete tail was observed on zebrafish juveniles (Figure 7A). These results suggested that **3** had low toxicity to zebrafish embryos, and such toxicity could extend the developmental period.[36]

CONCLUSIONS

A class of arene Ru(II) complexes, namely, [Ru(arene)(*p*-XPIP)]Cl where X = **1** (H), **2** (F), **3** (Cl), **4** (Br), and **5** (I), were synthesized by microwave-assisted heating technology. These complexes can bind and stabilize *c-myc* G-quadruplex

DOI: 10.1021/acs.organomet.5b00820
Organometallics XXXX, XXX, XXX−XXX

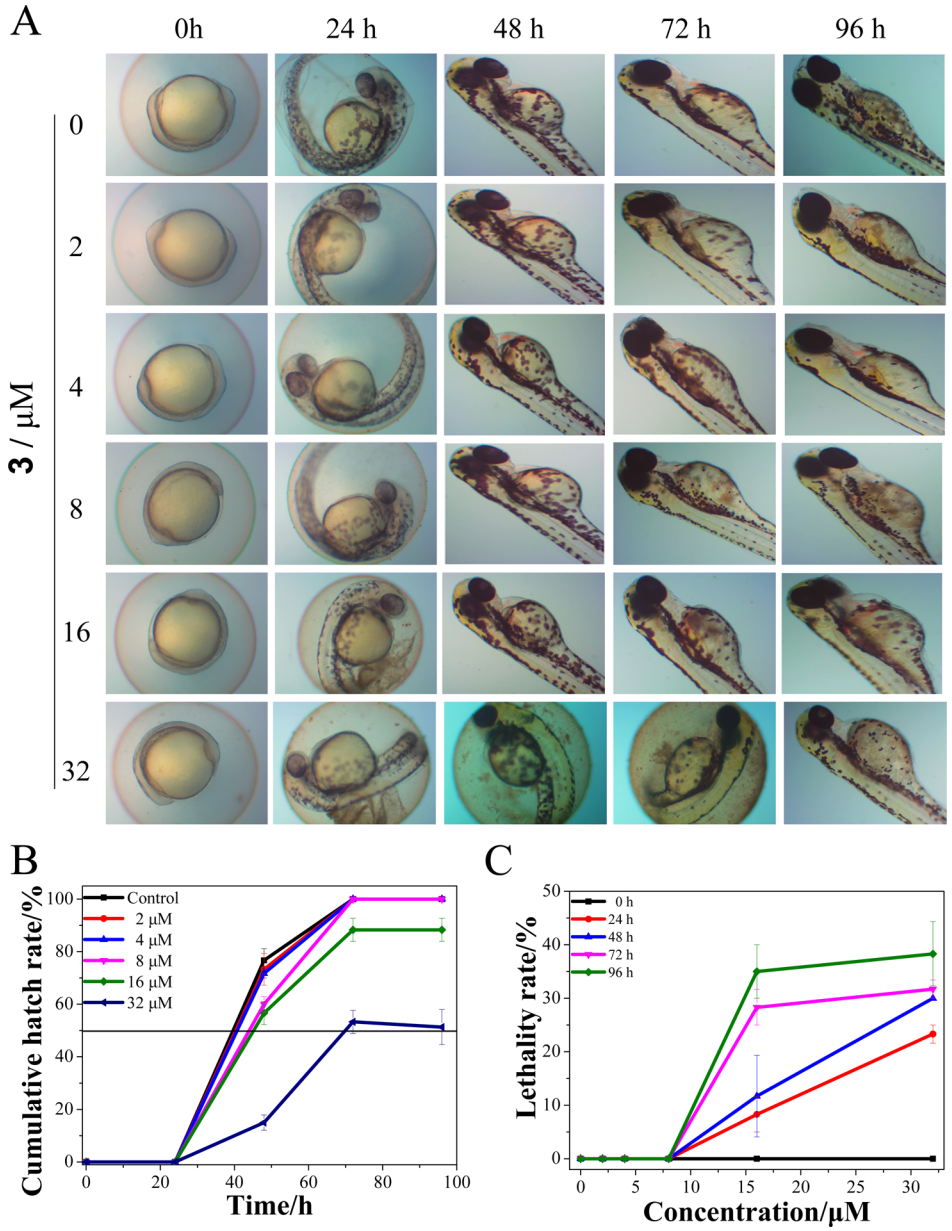

Figure 7. (A) Ecotoxicology of **3** to zebrafish embryo at different concentrations (0, 2, 4, 8, 16, and 32 μM) for 96 h on a 4× objective lens in the microscope. (B) Cumulative hatching rate of zebrafish embryos in the absence and in the presence of **3** (0, 2, 4, 8, 16, and 32 μM) every 24 h. (C) Lethality rate of zebrafish embryos in the absence and in the presence of **3** (0, 2, 4, 8, 16, and 32 μM) every 24 h.

DNA via the groove-binding mode. Results showed that these complexes, especially **3**, exhibited excellent inhibitory activity against proliferation, migration, and invasion of MDA-MB-231 breast cancer cells by acting on both S-phase arrest and apoptosis. The atomic size of the substituent in the main ligand played an important role in the determination of the level of inhibitory activity. In addition, the low toxicity of **3** on the development of zebrafish embryos was confirmed.

■ ASSOCIATED CONTENT

Supporting Information

The Supporting Information is available free of charge on the ACS Publications website at DOI: 10.1021/acs.organomet.5b00820.

The characterization data and X-ray crystal structure data of new compounds (PDF)

(CIF)

(CIF)

■ AUTHOR INFORMATION

Corresponding Authors

*Tel and Fax: +86-020-39352122. E-mail: yangqiuli@hotmail.com.

*E-mail: wenjiemei@126.com.

Notes

The authors declare no competing financial interest.

■ ACKNOWLEDGMENTS

The authors acknowledge the National Nature Science Foundation of China (Grant Number: 81572926), the Provincial Major Scientific Research Projects in Universities of Guangdong Province (Grant Number: 2014KZDXM053),

DOI: 10.1021/acs.organomet.5b00820
Organometallics XXXX, XXX, XXX−XXX

the Science and Technology Project of Guangdong Province (Grant Number: 2014A020212312), the Guangzhou City Science and Technology Plan (Grant Number: 2013J4100072), the Science and Technology Projects of Yuexiu District (Grant Number: 2014-WS-039), and the Joint Natural Sciences Fund of the Department of Science and Technology and the First Affiliated Hospital of Guangdong Pharmaceutical University (Grant Number: GYFYLH201309).

REFERENCES

(1) (a) Kumler, I.; Stenvang, J.; Moreira, J.; Brunner, N.; Nielsen, D. L. *Expert Rev. Anticancer Ther.* **2015**, *15*, 1075−1092. (b) Poole, V. L.; McCabe, C. J. *J. Endocrinol.* **2015**, *227*, R1−R12.

(2) Wang, P.; Cui, J.; Du, X.; Yang, Q.; Jia, C.; Xiong, M.; Yu, X.; Li, L.; Wang, W.; Chen, Y.; Zhang, T. *J. Ethnopharmacol.* **2014**, *154*, 663−671.

(3) Scolaro, C.; Bergamo, A.; Brescacin, L.; Delfino, R.; Cocchietto, M.; Laurenczy, G.; Geldbach, T. J.; Sava, G.; Dyson, P. J. *J. Med. Chem.* **2005**, *48*, 4161−4171.

(4) Bergamo, A.; Masi, A.; Peacock, A. F.; Habtemariam, A.; Sadler, P. J.; Sava, G. *J. Inorg. Biochem.* **2010**, *104*, 79−86.

(5) (a) Dai, Y.; Wilson, G.; Huang, B.; Peng, M.; Teng, G.; Zhang, D.; Zhang, R.; Ebert, M. P.; Chen, J.; Wong, B. C.; Chan, K. W.; George, J.; Qiao, L. *Cell Death Dis.* **2014**, *5*, e1170. (b) Yamada, Y.; Hidaka, H.; Seki, N.; Yoshino, H.; Yamasaki, T.; Itesako, T.; Nakagawa, M.; Enokida, H. *Cancer Sci.* **2013**, *104*, 304−312. (c) Yuan, L.; Tian, T.; Chen, Y.; Yan, S.; Xing, X.; Zhang, Z.; Zhai, Q.; Xu, L.; Wang, S.; Weng, X.; Yuan, B.; Feng, Y.; Zhou, X. *Sci. Rep.* **2013**, *3*, 1811.

(6) Hassani, L.; Fazeli, Z.; Safaei, E.; Rastegar, H.; Akbari, M. *J. Biol. Phys.* **2014**, *40*, 275−283.

(7) (a) Phan, A. T.; Kuryavyi, V.; Gaw, H. Y.; Patel, D. J. *Nat. Chem. Biol.* **2005**, *1*, 167−73. (b) Dai, J.; Carver, M.; Hurley, L. H.; Yang, D. *J. Am. Chem. Soc.* **2011**, *133*, 17673−17680. (c) Nanjunda, R.; Owens, E. A.; Mickelson, L.; Alyabyev, S.; Kilpatrick, N.; Wang, S.; Henary, M.; Wilson, W. D. *Bioorg. Med. Chem.* **2012**, *20*, 7002−7011.

(8) (a) Barry, N. P.; Abd Karim, N. H.; Vilar, R.; Therrien, B. *Dalton Trans.* **2009**, 10717−10719. (b) Therrien, B. *Eur. J. Inorg. Chem.* **2009**, *2009*, 2445−2453.

(9) Terenzi, A.; Bonsignore, R.; Spinello, A.; Gentile, C.; Martorana, A.; Ducani, C.; Högberg, B.; Almerico, A. M.; Lauria, A.; Barone, G. *RSC Adv.* **2014**, *4*, 33245−33256.

(10) Wu, Q.; He, J.; Mei, W.; Zhang, Z.; Wu, X.; Sun, F. *Metallomics* **2014**, *6*, 2204−2212.

(11) Fan, C.; Wu, Q.; Chen, T.; Zhang, Y.; Zheng, W.; Wang, Q.; Mei, W. *MedChemComm* **2014**, *5*, 597−602.

(12) Sun, D.; Wang, W.; Mao, J.; Mei, W.; Liu, J. *Bioorg. Med. Chem. Lett.* **2012**, *22*, 102−105.

(13) Wu, Q.; Chen, T.; Zhang, Z.; Liao, S.; Wu, X.; Wu, J.; Mei, W.; Chen, Y.; Wu, W.; Zeng, L. *Dalton Trans.* **2014**, *43*, 9216−9225.

(14) Sacher, M.; Jiang, Y.; Barrowman, J.; Scarpa, A.; Burston, J.; Zhang, L.; Schieltz, D.; Yates, J. R.; Abeliovich, H.; Ferro-Novick, S. *EMBO J.* **1998**, *17*, 2494−2503.

(15) Wu, Q.; Fan, C.; Chen, T.; Liu, C.; Mei, W.; Chen, S.; Wang, B.; Chen, Y.; Zheng, W. *Eur. J. Med. Chem.* **2013**, *63*, 57−63.

(16) Liu, Z. L.; Mao, J. H.; Peng, A. F.; Yin, Q. S.; Zhou, Y.; Long, X. H.; Huang, S. H. *Mol. Med. Rep.* **2013**, *7*, 608−612.

(17) Redondo-Muñoz, J.; Terol, M. J.; García-Marco, J. A.; García-Pardo, A. *Blood* **2008**, *111*, 383−386.

(18) Gallo, A.; Sterzo, C. L.; Mori, M.; Di Matteo, A.; Bertini, I.; Banci, L.; Brunori, M.; Federici, L. *J. Biol. Chem.* **2012**, *287*, 26539−26548.

(19) Zheng, Z. B.; Kang, S. Y.; Yi, X.; Zhang, N.; Wang, K. Z. *J. Inorg. Biochem.* **2014**, *141*, 70−78.

(20) (a) Zhou, J.; Yuan, G. *Chem. - Eur. J.* **2007**, *13*, 5018−5023. (b) David, W. M.; Brodbelt, J.; Kerwin, S. M.; Thomas, P. W. *Anal. Chem.* **2002**, *74*, 2029−2033.

(21) Gündel, U.; Kalkhof, S.; Zitzkat, D.; von Bergen, M.; Altenburger, R.; Küster, E. *Ecotoxicol. Environ. Saf.* **2012**, *76*, 11−22.

(22) Shi, W.; Song, S.; Zhang, H. *Chem. Soc. Rev.* **2013**, *42*, 5714−5743.

(23) Damas, A.; Chamoreau, L.-M.; Cooksy, A. L.; Jutand, A.; Amouri, H. *Inorg. Chem.* **2013**, *52*, 1409−1417.

(24) Boddupally, P. V.; Hahn, S.; Beman, C.; De, B.; Brooks, T. A.; Gokhale, V.; Hurley, L. H. *J. Med. Chem.* **2012**, *55*, 6076−6086.

(25) (a) Schobert, R.; Seibt, S.; Effenberger-Neidnicht, K.; Underhill, C.; Biersack, B.; Hammond, G. L. *Steroids* **2011**, *76*, 393−399. (b) Nazarov, A. A.; Baquie, M.; Nowak-Sliwinska, P.; Zava, O.; van Beijnum, J. R.; Groessl, M.; Chisholm, D. M.; Ahmadi, Z.; McIndoe, J. S.; Griffioen, A. W.; van den Bergh, H.; Dyson, P. J. *Sci. Rep.* **2013**, *3*, 1485.

(26) Sugiyama, Y.; Takabe, Y.; Nakakura, T.; Tanaka, S.; Koike, T.; Shiojiri, N. *Dev. Dyn.* **2010**, *239*, 386−397.

(27) (a) Clavel, C. M.; Paunescu, E.; Nowak-Sliwinska, P.; Griffioen, A. W.; Scopelliti, R.; Dyson, P. J. *J. Med. Chem.* **2015**, *58*, 3356−3365. (b) Nowak-Sliwinska, P.; van Beijnum, J. R.; Casini, A.; Nazarov, A. A.; Wagnieres, G.; van den Bergh, H.; Dyson, P. J.; Griffioen, A. W. *J. Med. Chem.* **2011**, *54*, 3895−3902. (c) Gligorijevic, N.; Arandelovic, S.; Filipovic, L.; Jakovljevic, K.; Jankovic, R.; Grguric-Sipka, S.; Ivanovic, I.; Radulovic, S.; Tesic, Z. *J. Inorg. Biochem.* **2012**, *108*, 53−61.

(28) Mazuryk, O.; Suzenet, F.; Kieda, C.; Brindell, M. *Metallomics* **2015**, *7*, 553−566.

(29) (a) Qin, Q. P.; Chen, Z. F.; Shen, W. Y.; Jiang, Y. H.; Cao, D.; Li, Y. L.; Xu, Q. M.; Liu, Y. C.; Huang, K. B.; Liang, H. *Eur. J. Med. Chem.* **2015**, *89*, 77−87. (b) Xu, X.; Li, J.; Sun, X.; Guo, Y.; Chu, D.; Wei, L.; Li, X.; Yang, G.; Liu, X.; Yao, L.; Zhang, J.; Shen, L. *Oncotarget* **2015**, *6*, 26161−26176. (c) Chen, Z. F.; Qin, Q. P.; Qin, J. L.; Zhou, J.; Li, Y. L.; Li, N.; Liu, Y. C.; Liang, H. *J. Med. Chem.* **2015**, *58*, 4771−4789. (d) Chen, Z. F.; Qin, Q. P.; Qin, J. L.; Liu, Y. C.; Huang, K. B.; Li, Y. L.; Meng, T.; Zhang, G. H.; Peng, Y.; Luo, X. J.; Liang, H. *J. Med. Chem.* **2015**, *58*, 2159−2179. (e) Xu, L.; Chen, X.; Wu, J.; Wang, J.; Ji, L.; Chao, H. *Chem. - Eur. J.* **2015**, *21*, 4008−4020.

(30) Ma, D.-L.; Chan, D. S.-H.; Fu, W.-C.; He, H.-Z.; Yang, H.; Yan, S.-C.; Leung, C.-H. *PLoS One* **2012**, *7*, e43278.

(31) (a) Khan, W. *J. Comput.-Aided Mol. Des.* **2011**, *25*, 81−101. (b) Xu, F.; Shi, X.; Li, S.; Cui, J.; Lu, Z.; Jin, Y.; Lin, Y.; Pang, J.; Pan, J. *Bioorg. Med. Chem.* **2010**, *18*, 1806−1815. (c) Li, J.; Xu, L.-C.; Chen, J.-C.; Zheng, K.-C.; Ji, L.-N. *J. Phys. Chem. A* **2006**, *110*, 8174−8180.

(32) (a) Zhang, Z.; He, X.; Yuan, G. *Int. J. Biol. Macromol.* **2011**, *49*, 1173−1176. (b) Bai, L. P.; Hagihara, M.; Nakatani, K.; Jiang, Z. H. *Sci. Rep.* **2014**, *4*, 6767.

(33) Yu, H.-j.; Zhao, Y.; Mo, W.-j.; Hao, Z.-f.; Yu, L. *Spectrochim. Acta, Part A* **2014**, *132*, 84−90.

(34) Chen, S.; Su, L.; Qiu, J.; Xiao, N.; Lin, J.; Tan, J.-h.; Ou, T.-m.; Gu, L.-q.; Huang, Z.-s.; Li, D. *Biochim. Biophys. Acta, Gen. Subj.* **2013**, *1830*, 4769−4777.

(35) (a) Agarwal, T.; Roy, S.; Chakraborty, T. K.; Maiti, S. *Biochemistry* **2010**, *49*, 8388−8397. (b) Ou, T.-M.; Lu, Y.-J.; Zhang, C.; Huang, Z.-S.; Wang, X.-D.; Tan, J.-H.; Chen, Y.; Ma, D.-L.; Wong, K.-Y.; Tang, J. C.-O. *J. Med. Chem.* **2007**, *50*, 1465−1474.

(36) Oehninger, L.; Stefanopoulou, M.; Alborzinia, H.; Schur, J.; Ludewig, S.; Namikawa, K.; Muñoz-Castro, A.; Köster, R. W.; Baumann, K.; Wölfl, S. *Dalton Trans.* **2013**, *42*, 1657−1666.

DOI: 10.1021/acs.organomet.5b00820
Organometallics XXXX, XXX, XXX−XXX